

# Effect of cyclic fatigue on the fracture toughness of Polyoxymethylene

B. Ramoa<sup>1</sup>, M. Berer<sup>1</sup>, M. Schwaiger<sup>1</sup>, G. Pinter<sup>2</sup>

<sup>1</sup> Polymer Competence Center Leoben GmbH, Leoben 8700, Austria

<sup>2</sup> Materials Science and Testing of Polymers, Montanuniversität Leoben, Leoben 8700, Austria

Correspondance to: bruno.ramoa@pccl.at

**Abstract.** Polymers are used in a wide range of applications and their properties are dependent upon the morphological development during processing and the specimen configuration which in turn define the mechanical properties. In this context fatigue and monotonic testing are part of the standard procedure to assess relevant mechanical and material parameters to ensure a better part design. The present work addresses the performance issues of a real component made of Polyoxymethylene (POM) which is subjected to cyclic loads from intermediate levels to high peak values inside a damping mechanism. For this linear elastic fracture mechanics concepts were used to characterize the behavior of a POM homopolymer resin used in this application. Injection molded compact tension specimens, with sharp and blunt notches, were tested under a combination of cyclic and monotonic loads and the fracture surfaces were examined. The critical stress intensity factor obtained by monotonic tests was evaluated as a function of the cycle number, where an increase after the first 1000 cycles followed by a continuous decrease with higher numbers of cycles was observed. A variation of approximately 50% and 70% were obtained along the duration of the tests for the sharp and blunt notch specimens, respectively. In light of the obtained results, a discussion is presented considering the dynamic specimen compliance and the structural features observed on the fracture surfaces in combination with the fracture mechanical response.

## 1. Introduction

Plastics are one of the most versatile materials in recent human history. They are used in a wide variety of applications, from agriculture to medicine, replacing in some cases ceramics and metals. Polyoxymethylene (POM) is a linear polymer composed of repeating  $-\text{CH}_2\text{-O}-$  units. This material is used in many structural applications such as gears, sliding components and bearings due to its tribological properties, stiffness, dimensional stability and fatigue resistance [1–5].

In service application polymer components are frequently exposed to several combinations of loads during their life. Under cyclic loadings, polymeric structures can fail at load levels lower than they can withstand under monotonic situations [6]. Hence, there is a need to understand the effect of fatigue on the mechanical properties of the materials to ensure a better part design. Nowadays, fatigue and monotonic fracture testing are common procedures to assess relevant mechanical and material parameters. For their analysis different concepts of fracture mechanics can be applied to polymers depending on the test temperature, strain rate, specimen configuration and instrumental setup which in turn dictate the fracture behavior of a material. For POM, the concept of crack tip opening displacement



[7], essential work of fracture [8] and linear elastic fracture mechanics (LEFM) [9–11] have already been applied. There are some studies regarding the fatigue and monotonic fracture behavior of POM [9, 10, 12–14]. However, the effect of cyclic fatigue on the critical stress intensity factor for the chosen material and specimen configuration, to the best of authors' knowledge, has not yet been studied. There is one article which studies this effect for polycarbonate [15] but usually the influence of fatigue on the tensile properties rather than on the fracture toughness is addressed in the literature [12, 16, 17].

This work explores the fracture toughness of a commercial Polyoxymethylene homopolymer used to manufacture a thin-walled component. The component and the issue observed in service application are depicted in Figure 1. The component is used as part of a damping system which is composed of a piston and a cylinder with fluid inside. In application, this device is loaded monotonically with the compression of the fluid and it suffers fatigue with multiple usage. It was noticed that, after some cycles at medium to large load levels, the strength of the cylinder was noticeably reduced which caused a crack to be developed near the notch of the cylinder. The crack development process was rather spontaneous and hence was not considered as fatigue crack growth. To study this effect on specimen level, injection molded compact tension (CT) specimens were used and submitted to cyclic fatigue followed by monotonic quasi-static tensile testing.

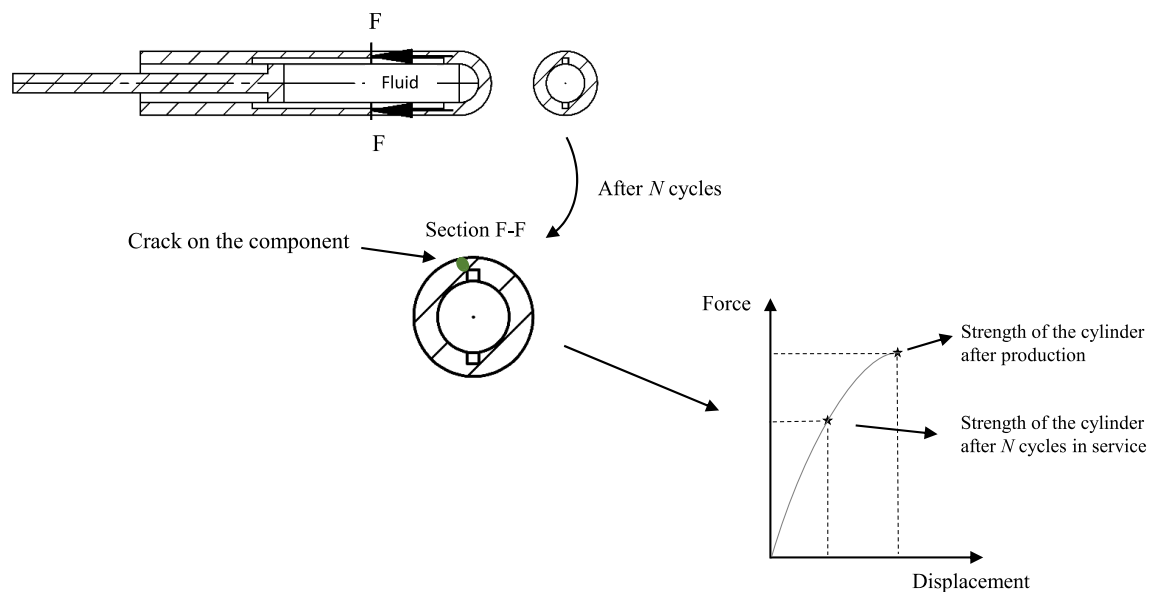


Figure 1: Schematic representation of the damping system and definition of the problem observed in service application

## 2. Experimental

### 2.1. Material and Specimen

The material used during this research was a commercially available Polyoxymethylene homopolymer resin produced by DuPont (DuPont, Wilmington, DE). The resin represents a modified version of “Delrin 300”. From the manufacturer’s datasheet some relevant properties are summarized in Table 1.

Table 1: Relevant material properties from the manufacturer’s datasheet.

Property	Value	Unit
Density (ISO 1183)	1.42	$\text{g/cm}^3$
Melt Flow Rate (ISO 1133)	6	$\text{cm}^3/10 \text{ min}$
Melting Temperature (ISO 11357)	178	$^\circ\text{C}$
Yield Stress (ISO 527)	71	MPa
Tensile Modulus (ISO 527)	3.1	GPa

The fracture mechanics tests were performed on injection molded compact tension specimens with a width ( $W$ ) of 40 mm and a thickness of 4 mm. Further details of the geometry are given in Figure 2. All the specimens were molded with the same processing conditions and in one production process.

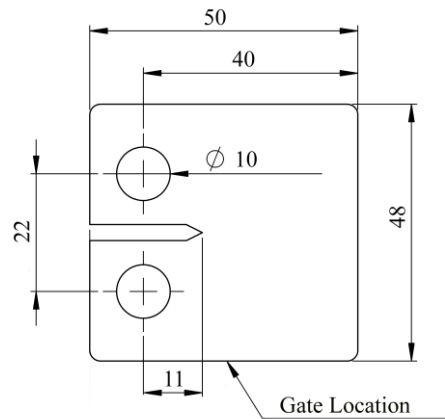


Figure 2: Compact tension test specimen following [18]

In order to assure plane strain conditions the size criteria given in Equation 1 should be met [18]. However, with the yield stress in Table 1 and the fracture toughness results in Table 2 this leads to a minimum required thickness of approximately 9 mm which is much higher than the 4 mm thick CT specimens used in this study. Hence, the test configuration does not ensure that the determined critical stress intensity factors are material properties and the denomination “ $K_C$ ” is used instead of “ $K_{IC}$ ”. Nevertheless, the determined  $K_C$  values should suffice for comparing samples with the same geometry.

$$B, a, (W - a) \geq 2.5 \left( \frac{K_C}{\sigma_Y} \right)^2 \quad (1)$$

Where  $\sigma_Y$  is the yield stress of the material,  $B$  the thickness and  $a$  the crack length

## 2.2. Fracture mechanics tests

The CT specimens were analyzed in two ways. One set of samples was notched prior to testing using a fresh portion of a thin razor blade. This was done to guarantee a uniform crack geometry with approximately 1-2 mm in depth. The second set was used as obtained from the injection molding process. The latter had a blunt notch that better represented the notch geometry of the component where the cracks were observed in the service application. For purposes of comparison, the first set of samples will be termed “Blade Notch” and the second set will be termed “Injection Molded Notch” or “IM Notch” for short.

The fatigue and monotonic fracture tests were performed on a servo-hydraulic testing machine of the type “MTS 858 horizontal” (MTS, Eden Prairie, MN, USA) in load controlled mode. The fatigue measurements were performed in tension with a sinusoidal signal of 10 Hz and a load ratio,  $R$  ( $F_{min}/F_{max}$ ) of 0.1. To observe the actual crack length of the specimens a traveling microscope with a magnification of 20 (lens: Marcel Aubert SA, Bienne, Switzerland; adjustable desk: Mitutoyo, Tokyo, Japan) was mounted on the testing device. It is known that in the mechanically dominated fatigue region the fatigue life is highly dependent on the amplitude and frequency of loading. During this study, the experiments were conducted assuming plausible service conditions, i.e., maximum and minimum force of 450 and 45 N, respectively. The peak/valley pairs of force and displacement were recorded every 100 cycles, and every 1000 cycles complete hysteresis curves were recorded. The selected load level shows a rather

limited life time in fatigue fracture tests (ca.  $3 \times 10^5$  cycles). Additionally it is expected that this load level causes comparably big zones of irreversible deformation in the fatigue tests which was intended because it is expected to better represent the conditions in the real component. As mentioned above the formation of the cracks in the real component (Figure 1) happened rather spontaneous. Thus, it was expected that irreversible deformation played a significant role in the fatigue process of the cylinder.

The force and displacement pairs recorded every 100 cycles were used to calculate the dynamic specimen compliance, following Equation 2. This parameter has been found to be quite useful for mechanical studies during fatigue tests. Previously it was used to generate fatigue crack growth kinetics curves of POM and PEEK [9, 10] and to minimize the influence of creep on the dynamic mechanical analyses of fatigue tests [17, 19].

$$C_{Dym} = |C^*| = \frac{d_{max} - d_{min}}{F_{max} - F_{min}} \quad (2)$$

Where  $C_{Dym}$  is the dynamic compliance which is equivalent to the magnitude of the complex specimen compliance.  $d_{max}$  and  $d_{min}$  are the peak/valley data of the displacement and  $F_{max}$  and  $F_{min}$  the corresponding force data.

After fatiguing for  $10^3$ ,  $10^4$  and  $10^5$  cycles, the tests with fatigue pre-load were stopped for one minute followed by a monotonic tensile test with a piston velocity of 10 mm/min. From the force – displacement curves, the maximum force was used to estimate the stress intensity factor using Equation 3 [18]. Additionally, monotonic fracture tests on unfatigued samples were conducted. For each testing condition at least 5 specimens were used.

$$K_C = \frac{F}{B\sqrt{W}} f\left(\frac{a}{W}\right) \quad (3)$$

$$f\left(\frac{a}{W}\right) = \frac{2 + \frac{a}{W}}{\left(1 - \frac{a}{W}\right)^{\frac{3}{2}}} \left[ 0.886 + 4.64 \left(\frac{a}{W}\right) - 13.32 \left(\frac{a}{W}\right)^2 + 14.72 \left(\frac{a}{W}\right)^3 - 5.60 \left(\frac{a}{W}\right)^4 \right]$$

Where  $K_C$  is the critical stress intensity factor in mode I,  $F$  the maximum load and  $W$  the width

### 2.3. Light Microscopy

The cross section of the post-mortem representative specimens were studied under light microscopy in reflection mode using an ‘‘Olympus SZX12’’ microscope (Olympus Corporation, Tokyo, Japan) with a magnification of 25. The dimensions of the plastic zones and of discontinuous crack growth bands (DCG) were measured using the measuring tools of the integrated image acquisition software.

## 3. Results and Discussion

The effect of cyclic pre-loading on the measured critical stress intensity factor is shown in Figure 3. The corresponding values are given in Table 2. For the measurements with the highest number of pre-cycles ( $10^5$  cycles) it was observed that crack growth initiation had already started. In this case  $K_C$  was corrected for the higher crack length using post-mortem micrographs and assuming that the increment in crack length was equal to the width of the DCG band. In order to assess the effect of the relaxation time, one additional test was carried out for each fatigue condition on the Blade Notch CT specimens. This time the test was stopped for 15 minutes between the cyclic pre-loading and the monotonic fracture test. The corresponding results are also included in Figure 3 and Table 2.

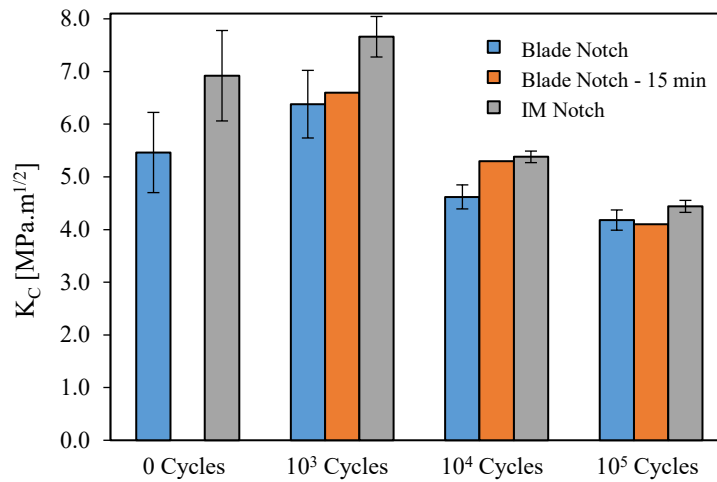


Figure 3: Evolution of  $K_C$  with increasing number of cycles in the fatigue pre-loading step

Analysis of Figure 3 indicates that both specimen types examined (Blade Notch and IM Notch) have the same trend which is important concerning the conclusions for the real component. The measured critical stress intensity factor increases for the first  $10^3$  cycles of fatigue followed by a continuous decrease afterwards. Considering the maximum and minimum values obtained, there is a relative variation in the critical stress intensity factor ( $(K_{C \text{ Max}} - K_{C \text{ Min}}) / K_{C \text{ Min}}$ ) of approximately 50% for the Blade Notch and of approximately 70% for the IM Notch specimens. For the IM Notch specimens, the average  $K_C$  values determined are always higher than the ones obtained for the Blade Notch ones. The specimens of the latter type have a sharper crack radius therefore the stress is more concentrated at the crack tip and less energy is needed to initiate crack growth. Interestingly, the difference decreases with increasing number of fatigue cycles which is attributed to the development of well-defined craze zones with similar geometric characteristics.

The samples tested with a relaxation time of 15 minutes display the same trend and similar values as the ones with 1 minute relaxation time thus one can assume that, for the chosen setup, relaxation has a low effect on  $K_C$ . Moreover, because of the long relaxation time of 15 min it can also be excluded that the changes in the  $K_C$  values are a thermal effect (due to hysteretic heating during fatigue pre-loading).

Table 2: Average values of the critical stress intensity factor measured for each testing condition

Number of fatigue cycles (N)	0	10 <sup>3</sup>	10 <sup>4</sup>	10 <sup>5</sup>
$K_C$ (Blade Notch) [ $\text{MPa}\cdot\text{m}^{1/2}$ ]	5.5 ± 0.76	6.4 ± 0.64	4.6 ± 0.23	4.2 ± 0.19
$K_C$ (Blade Notch -15min) [ $\text{MPa}\cdot\text{m}^{1/2}$ ]	-	6.6	5.3	4.1
$K_C$ (IM Notch) [ $\text{MPa}\cdot\text{m}^{1/2}$ ]	6.9 ± 0.86	7.7 ± 0.38	5.4 ± 0.11	4.4 ± 0.11

A representative force-displacement curve for each testing condition is presented in Figure 4. All samples reveal brittle behavior. It can also be seen that both force and displacement values decrease with increasing number of fatigue cycles as was observed in service application for the component. The effect is more pronounced for the blunt specimens than for the sharp notched ones.

Table 3: Estimated and measured dimension of plastic zones of specimens without fatigue pre-load

Blade Notch			IM Notch		
$d_{\text{plane strain}}$ (mm)	$d_{\text{plane stress}}$ (mm)	$d_{\text{observed}}$ (mm)	$d_{\text{plane strain}}$ (mm)	$d_{\text{plane stress}}$ (mm)	$d_{\text{observed}}$ (mm)
0.63	1.88	0.16	1.01	3.02	0.34

Irreversible material deformation, such as crazing in polymers, leads to stress relaxation at the crack tip. The LEFM approach becomes more inaccurate as this plastic region at the crack tip grows. For the monotonous tests without fatigue pre-load the size of the plastic zone ( $d$ ) was estimated using Equation 4 and 6, for plane strain conditions, and Equation 5 and 6, for plane stress conditions [20]. For the calculations, the yield stress in Table 1 and the  $K_C$  values in Table 2 were used. Micrographs of the corresponding unfatigued specimens of both notch conditions were used to assess the size of the plastic zone. For these specimens the measured  $d$  values are reported in Table 3. They indicate the presence of a lower plastic zone than the ones estimated with Equation 6. Hence, at least for the monotonous tests without fatigue pre-load pure plane strain conditions can be assumed. For the specimens with fatigue pre-load this analysis could not be conducted because in this case the plastic zone dimensions were strongly influenced by the fatigue process.

$$r_{plane\ strain} = \frac{1}{6\pi} \left( \frac{K_C}{\sigma_Y} \right)^2 \quad (4)$$

$$r_{plane\ stress} = \frac{1}{2\pi} \left( \frac{K_C}{\sigma_Y} \right)^2 \quad (5)$$

$$d = 2r \quad (6)$$

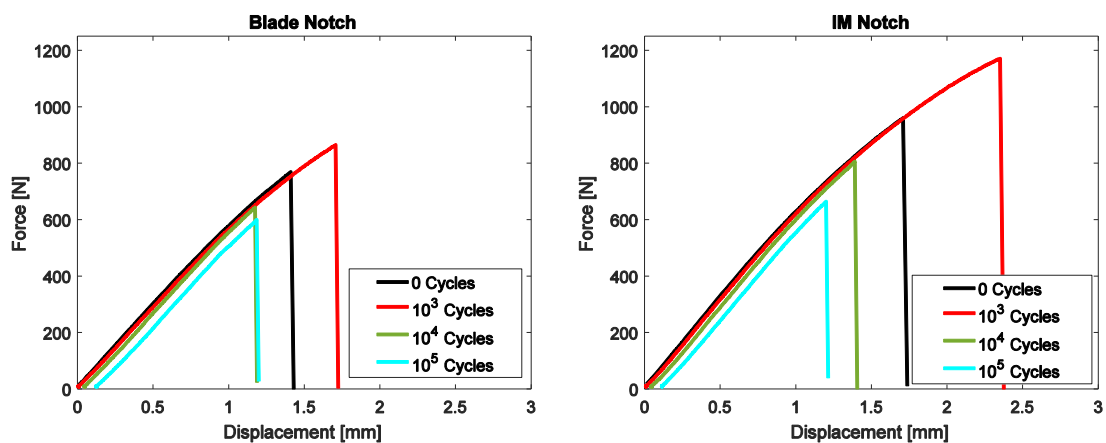


Figure 4: Representative force-displacement curves of Blade Notch (left) and IM Notch (right) specimens for each testing condition

For the sake of completeness, the dynamic compliance and hysteresis curves of a representative specimen fatigued for  $10^5$  cycles are presented in Figure 5 and 6 for each notch type used. For the Blade Notch specimen  $C_{Dyn}$  decreases slightly until right after  $2 \times 10^4$  cycles followed by a plateau and a sudden jump. Regarding the IM Notch specimen, a slight decrease in the compliance is also visible followed by several stair-like jumps. Berer et al., [9] studied fatigue crack growth of POM using the dynamic compliance method. They noticed a decrease in the initial portion of the dynamic compliance followed by a small jump for blade notched CT specimens. The authors attributed this to the formation of a craze zone and the subsequent drawing of fibrils which made the material stiffer thus reducing the compliance of the specimen. As for the following jump, it was attributed to the fracture of fatigued fibrils and to the initiation of crack growth. It is worth noting that in the present study cyclic fatigue was performed until a maximum of  $1 \times 10^5$  cycles, which, for the experimental setup used, represents a region slightly after crack growth initiation. Thus only slight changes are visible in the specimens' compliances shown in Figure 5. For comparison purposes the complete dynamic compliance curve of a cyclic fatigue test conducted until fracture is included in Figure 5 for a Blade Notch sample. From the insert in Figure 5 it

can be seen that the maximum number of cycles ( $10^5$ ) used for the fatigue pre-loading represents about one-third of the fatigue life time for the chosen setup and load level ( $F_{\max}$  450 N /  $F_{\min}$  45 N).

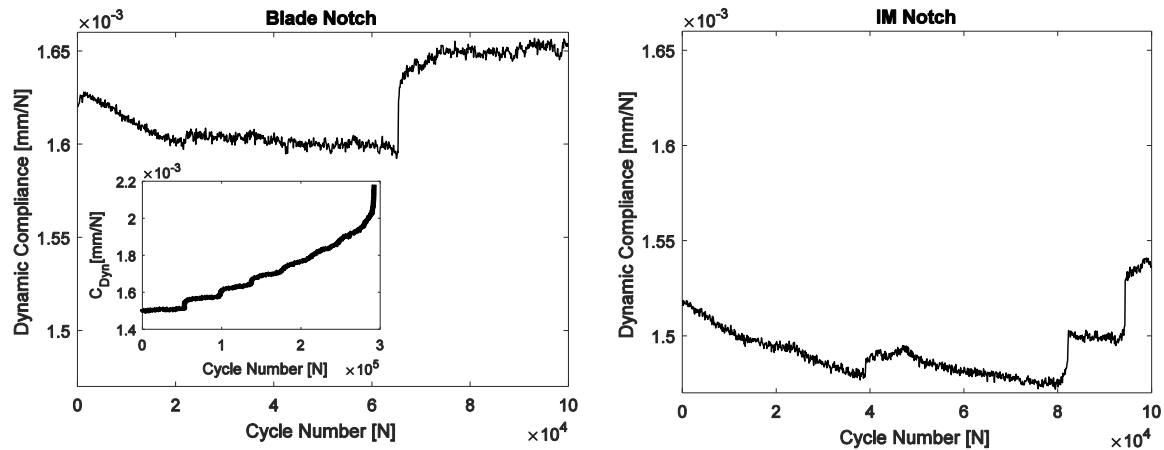


Figure 5: Dynamic compliance curve for the Blade Notch (left) and IM Notch (right) specimens with  $10^5$  cycles of fatigue pre-load (the insert in the plot to the left shows a complete fatigue fracture test with identical setup and load level)

The hysteresis curves shown in Figure 6 are very similar in shape but shifted rightwards with increasing number of fatigue cycles. The similarity in shape indicates that the dynamic mechanical behavior of the specimen is quite similar for the three different numbers of cycles used for the fatigue pre-load. The shift in displacement with cycle number can be attributed to the viscoelastic deformation (creep) coupled with crack growth for the highest cycle number shown. The latter is also indicated by a small decrease in the slope of the corresponding hysteresis curves. The hysteresis data were also used to split the dynamic compliance into its storage and loss parts as well as to calculate the loss factor. However, no significant differences could be detected and thus the results are not shown here.

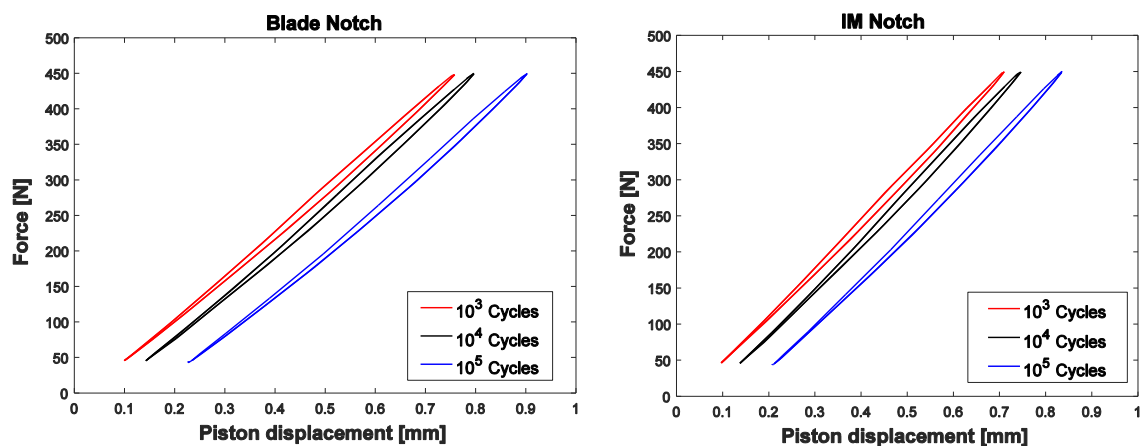


Figure 6: Hysteresis loops of Blade Notch (left) and IM Notch (right) specimens during the fatigue pre-load up to  $10^5$  cycles

Images of the fracture surfaces obtained by light microscopy are presented in Figure 7. For each testing condition a representative specimen was selected. It can be seen that all micrographs, depending on the amount of cyclic fatigue, present some level of stress whitening. From 0 to  $10^4$  cycles of fatigue pre-load all images show the same basic features. On the micrographs four distinct regions can be observed for the Blade Notch specimens and three for the IM Notch specimens (numbered from left to right). For the Blade Notch specimens, region one and two represent the notch from the manufacturing process and the one introduced by the blade, respectively. Region three will be termed as “plastic zone”

in the following discussion. It is formed by the coupled effect of cyclic fatigue and monotonic loading. Finally region four corresponds to spontaneous crack growth at the end of the monotonic tests. The surface of this region indicates that the specimen broke in a brittle manner without further plastic deformation. For the IM Notch specimens, region one represents the notch from the molding process. Region two and three are homologous to regions 3 and 4 of the Blade Notch specimens. Comparing the samples with and without fatigue pre-load it is obvious that the size of the plastic zone is bigger for the specimens with fatigue pre-load.

For the specimens with  $10^5$  cycles of fatigue pre-load, four and five different regions can be distinguished for the blunt and sharp notched specimens, respectively. Additionally to the previously discussed ones, the plastic zone is divided into two parts. The boundary between these two parts is interpreted as a discontinuous crack growth band. These are formed when a fatigue crack remains static for some period of cyclic loading in which a craze at the crack tip grows and matures. With further increase in cycle number, a sudden advance in the crack length occurs and the procedure is repeated until either unstable crack growth takes place or the mechanism changes to continuous crack growth [21, 22]. Images very similar to the ones presented here can also be found in [9], where the authors attributed the white color of the plastic zones to the formation of micro-voids that were generated during craze formation. This is supported by Plummer et al [23, 24] who observed that the yielding behavior in bulk POM was accompanied by stress whitening and cavitation.

Based on the compliance curves and the light microscope images it is interpreted that the increase in  $K_C$  during the first 1000 cycles is caused by the formation of a distinct craze zone with fibrils, which draws material from the polymer matrix resulting in a localized strain hardening. After a certain number of cycles the strain hardening effect produced by the fibril formation and orientation is counterpoised by the coalescence of voids (which were nucleated during the fibril formation) and by disentanglement and / or fracture of highly stressed fibrils [22, 23].

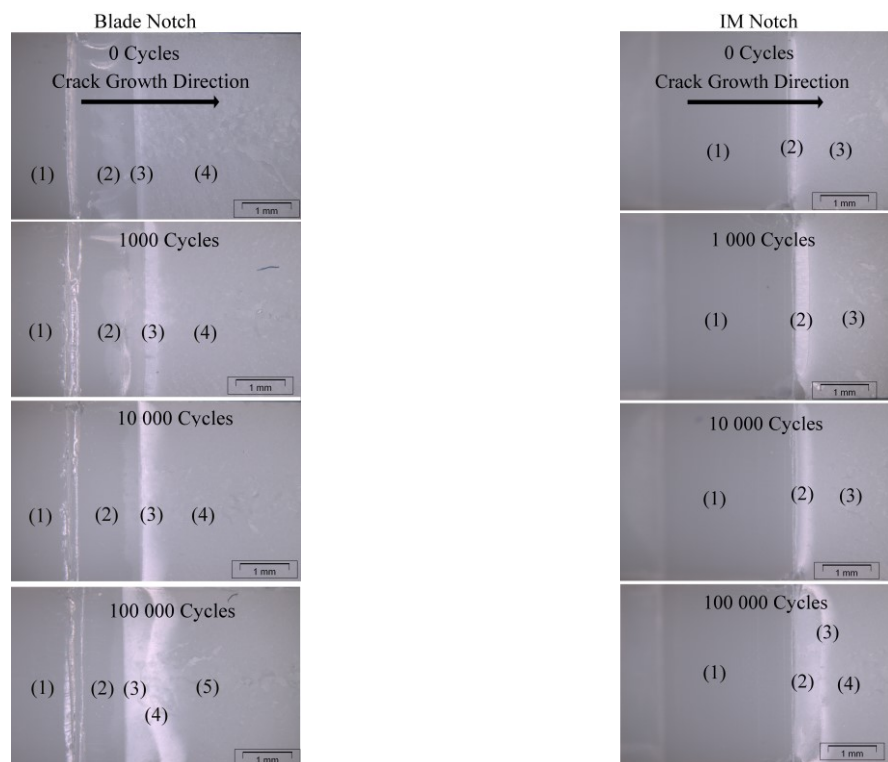


Figure 7: Sequence of fracture surfaces for both Blade Notch and IM-Notch specimens obtained for different levels of fatigue pre-load conditions

#### 4. Conclusions

The effect of cyclic fatigue on the fracture toughness of Polyoxymethylene was investigated. The results were discussed in light of previous findings available in the literature. It was observed, within the experimental conditions used, that the critical stress intensity factor increases at low fatigue cycle numbers but strongly decreases with further fatigue loading. Supported by micrographs and plots of the dynamic specimen compliance, this was attributed to the formation and fatigue of a craze zone ahead of the crack tip. For low numbers of fatigue cycles the dominant effect was local strain hardening produced by drawing and orientation of fibrils. With further increasing fatigue the coalescence of voids and the breakdown of fibrils in the craze zone caused the critical stress intensity factor and thus the fracture toughness of the material to significantly decrease. Along the performed measurements a variation in the stress intensity factor of nearly 50% for the blade notched specimens and of 70% for the blunt notched specimens was observed.

The conclusion for the component is that the design of notched areas has to take into account the reduction of the fracture toughness in service applications when fatigue loading is present. Currently this mainly affects thin walled parts in combination with the material (Polyoxymethylene homopolymer) examined in this study. However, the formation and fatigue of craze zones is not an effect which was only observed for Polyoxymethylene. This effect is present in all polymers which show discontinuous crack growth bands in fracture mechanical fatigue tests [22].

#### Acknowledgements

The research work of this article was performed at the Polymer Competence Center Leoben GmbH (PCCL, Austria) within the framework of the COMET-programme of the Austrian Ministry of Traffic, Innovation and Technology with contributions by the Montanuniversität Leoben (Materials Science and Testing of Plastics). The PCCL is funded by the Austrian Government and the State Governments of Styria and Upper Austria.

#### References

- [1] S. Lüftl, P. M. Visakh, and S. Chandran, 2014, *Polyoxymethylene Handbook : Structure, Properties, Applications and their Nanocomposites*: Wiley pp.153-163.
- [2] M. Berer and Z. Major, 2010, "Characterization of the global deformation behaviour of engineering plastics rolls," *Int. J. Mech. Mater. Des.*, **6**, pp. 1–9.
- [3] M. Berer and Z. Major, 2012, "Characterisation of the Local Deformation Behaviour of Engineering Plastics Rolls," *Strain*, **48**, pp. 225–234.
- [4] Heym B. and Beitz W., 1995, "Zur Belastbarkeit von Stirnzahnrädern aus dem Hochtemperatur-Thermoplast PEEK," *Konstruktion*, **47**, pp. 351–357.
- [5] J. Rösler, 2005, "Zur Tragfähigkeitssteigerung thermoplastischer Zahnräder mit Füllstoffen," Dissertation, Fakultät V der Technische Universität Berlin, Berlin, Germany.
- [6] J. A. Sauer and G. C. Richardson, 1980, "Fatigue of polymers," *Int. Journ. of Fracture*, **16**, pp. 499–532.
- [7] C. J. G. Plummer, P. Scaramuzzino, H.-H. Kausch, and J.-M. Philippoz, 2000, "High temperature slow crack growth in polyoxymethylene," *Polym. Eng. Sci.*, **40**, pp. 1306–1317.
- [8] C. J. G. Plummer, P. Scaramuzzino, R. Steinberger, R. W. Lang, and H.-H. Kausch, 2000, "Application of the essential work of fracture concept to high temperature deformation in polyoxymethylene," *Polym. Eng. Sci.*, **40**, pp. 985–991.
- [9] M. Berer, G. Pinter, and M. Feuchter, 2014, "Fracture mechanical analysis of two commercial polyoxymethylene homopolymer resins," *J. Appl. Polym. Sci.*, **131**, 40831.
- [10] M. Berer and G. Pinter, 2013, "Determination of crack growth kinetics in non-reinforced semi-crystalline thermoplastics using the linear elastic fracture mechanics (LEFM) approach," *Polym. Test.*, **32**, pp. 870–879.

- [11] F. Arbeiter, B. Schritteser, A. Frank, M. Berer, and G. Pinter, 2015, "Cyclic tests on cracked round bars as a quick tool to assess the long term behaviour of thermoplastics and elastomers," *Polym. Test.*, **45**, pp. 83–92.
- [12] A. Lazzeri, A. Marchetti, and G. Levita, 1997, "Fatigue and Fracture in Polyacetal Resins," *Fatigue Fract. Eng. Mater. Struct.*, **20**, pp. 1207–1216.
- [13] A. J. Lesser, 1995, "Changes in Mechanical Behavior During Fatigue of Semicrystalline Thermoplastics," *J. Appl. Polym. Sci.*, **58**, pp. 869–879.
- [14] S. Bandyopadhyay, J. R. Roseblade, and R. Muscat, 1993, "Fracture study of a polyacetal resin," *J. Mater. Sci.*, **28**, pp. 3777–3782.
- [15] X. Li, H. A. Hristov, A. F. Yee, and D. W. Gidley, 1995, "Influence of cyclic fatigue on the mechanical properties of amorphous polycarbonate," *Polymer*, **36**, pp. 759–765.
- [16] Q.-Z. Fang, T. J. Wang, H. G. Beom, and H. M. Li, 2008, "Effect of cyclic loading on tensile properties of PC and PC/ABS," *Polym. Degrad. Stab.*, **93**, pp. 1422–1432.
- [17] M. Berer, Z. Major, G. Pinter, D. M. Constantinescu, and L. Marsavina, 2014, "Investigation of the dynamic mechanical behavior of polyetheretherketone (PEEK) in the high stress tensile regime," *Mech Time-Depend Mater*, **18**, pp. 663–684.
- [18] ISO 13586, 2000, Plastics — Determination of fracture toughness ( $G_{IC}$  and  $K_{IC}$ ) — Linear elastic fracture mechanics (LEFM) approach.
- [19] M. Berer, D. Tscharnuter, and G. Pinter, 2015, "Dynamic mechanical response of polyetheretherketone (PEEK) exposed to cyclic loads in the high stress tensile regime," *Int. J. Fatigue*, **80**, pp. 397–405.
- [20] H. Tada, P. C. Paris, and G. R. Irwin, 2000, The stress analysis of cracks handbook, 3rd ed. New York: ASME Press; London : Professional Engineering Publishing pp.16.
- [21] P. E. Bretz, R. W. Hertzberg, and J. Manson, 1982, "The Effect of Molecular Weight on Fatigue Crack Propagation in Nylon 66 and Polyacetal," *J. Appl. Polym. Sci.*, **27**, pp. 1707–1717.
- [22] R. W. Hertzberg and J. A. Manson, 1980, Fatigue of Engineering Plastics: Academic Press pp.146-183.
- [23] C. J. G. Plummer, N. Cudré-Mauroux, and H.-H. Kausch, 1994, "Deformation and Entanglement in Semicrystalline Polymers," *Polym. Eng. Sci.*, **34**, pp. 318–329.
- [24] C. J. G. Plummer, P. Menu, N. Cudré-Mauroux, and H.-H. Kausch, 1995, "The Effect of Crystallization Conditions on the Properties of Polyoxymethylene," *J. Appl. Polym. Sci.*, **55**, pp. 489–500.